Molecular Therapy
Methods & Clinical Development
Original Article

Spatially and Temporally Regulated *NRF2* Gene Therapy Using *Mcp-1* Promoter in Retinal Ganglion Cell Injury

Kosuke Fujita,[1] Koji M. Nishiguchi,[2] Yukihiro Shiga,[3] and Toru Nakazawa[1,2,3]

[1]Department of Retinal Disease Control, Tohoku University Graduate School of Medicine, Sendai 980-8574, Japan; [2]Department of Advanced Ophthalmic Medicine, Tohoku University Graduate School of Medicine, Sendai 980-8574, Japan; [3]Department of Ophthalmology, Tohoku University Graduate School of Medicine, Sendai 980-8574, Japan

Retinal ganglion cell degeneration triggered by axonal injury is believed to underlie many ocular diseases, including glaucoma and optic neuritis. In these diseases, retinal ganglion cells are affected unevenly, both spatially and temporally, such that healthy and unhealthy cells coexist in different patterns at different time points. Herein, we describe a temporally and spatially regulated adeno-associated virus gene therapy aiming to reduce undesired off-target effects on healthy retinal neurons. The Mcp-1 promoter previously shown to be activated in stressed retinal ganglion cells following murine optic nerve injury was combined with the neuroprotective intracellular transcription factor *Nrf2*. In this model, Mcp-1 promoter-driven NRF2 expression targeting only stressed retinal ganglion cells showed efficacy equivalent to non-selective cytomegalovirus promoter-driven therapy for preventing cell death. However, cytomegalovirus promoter-mediated *NRF2* transcription induced cellular stress responses and death of Brn3A-positive uninjured retinal ganglion cells. Such undesired effects were reduced substantially by adopting the Mcp-1 promoter. Combining a stress-responsive promoter and intracellular therapeutic gene is a versatile approach for specifically targeting cells at risk of degeneration. This strategy may be applicable to numerous chronic ocular and non-ocular conditions.

INTRODUCTION

Glaucoma, characterized by progressive loss of retinal ganglion cells (RGCs), is one of the leading causes of blindness worldwide. It is a multifactorial disease, although elevated intraocular pressure (IOP) remains the only proven therapeutic target. In glaucoma and many other ocular conditions, RGC death can occur unevenly across the retina such that stressed cells and healthy cells reside next to each other in a pattern that varies over time.[1] Oxidative stress is an important factor in glaucoma pathogenesis. A large body of evidence from analysis of patient's biological samples[2–5] and animal models has established a strong link between glaucoma and elevated oxidative stress markers, both dependent on IOP[6,7] and independent of IOP.[8,9]

Adeno-associated virus (AAV) gene therapy allowing long-term expression of a therapeutic gene is a promising approach to treat chronic ocular conditions. In all AAV-mediated ocular gene therapy trials published to date,[10–14] a constitutively active promoter, chicken β-actin promoter, was chosen to drive the transgene to maximize expression, except for a trial in which the human RPE65 promoter was used.[11] However, such promoters result in unregulated expression of the therapeutic gene in all AAV-transduced cells, including both injured and healthy cells that may coexist within the same retina. This could induce stress responses by triggering a non-physiological condition in the healthy ones. To circumvent this problem, tissue- or cell-specific promoters have been used to restrict expression of the target (therapeutic) gene to cell types at risk of damage.[11] While this strategy helps to direct transgene expression to the target cell type, it is of limited use for conditions in which healthy and unhealthy cells are mixed within that population. We studied the temporal transcription profiles of various stress pathway-related promoters and response elements in RGCs using AAV2-based reporters in a murine optic nerve crush (ONC) model.[15] Through this work, we identified the monocyte chemoattractant protein 1 (Mcp-1) promoter involved in leukocyte recruitment[16] as being capable of driving reporter gene expression in stressed RGCs preceding their death with relatively low background activity. The therapeutic utility of AAV-mediated delivery of NRF2, a transcription factor inducing the expression of multiple antioxidant genes,[17] for treating RGCs was demonstrated in a murine model of ONC.[18] However, as the study used a constitutive cytomegalovirus (CMV) promoter connected to a human β-globulin intron to drive NRF2 expression, concern regarding off-target effects on neighboring healthy RGCs remained.

In the current study, we explored the therapeutic utility of combining the Mcp-1 promoter with the transcription factor gene

Received 27 December 2016; accepted 12 April 2017;
http://dx.doi.org/10.1016/j.omtm.2017.04.003.

Correspondence: Koji M. Nishiguchi, Tohoku University Graduate School of Medicine, Sendai 980-8574, Japan.
E-mail: nishiguchi@oph.med.tohoku.ac.jp
Correspondence: Toru Nakazawa, Tohoku University Graduate School of Medicine, Sendai 980-8574, Japan.
E-mail: ntoru@oph.med.tohoku.ac.jp

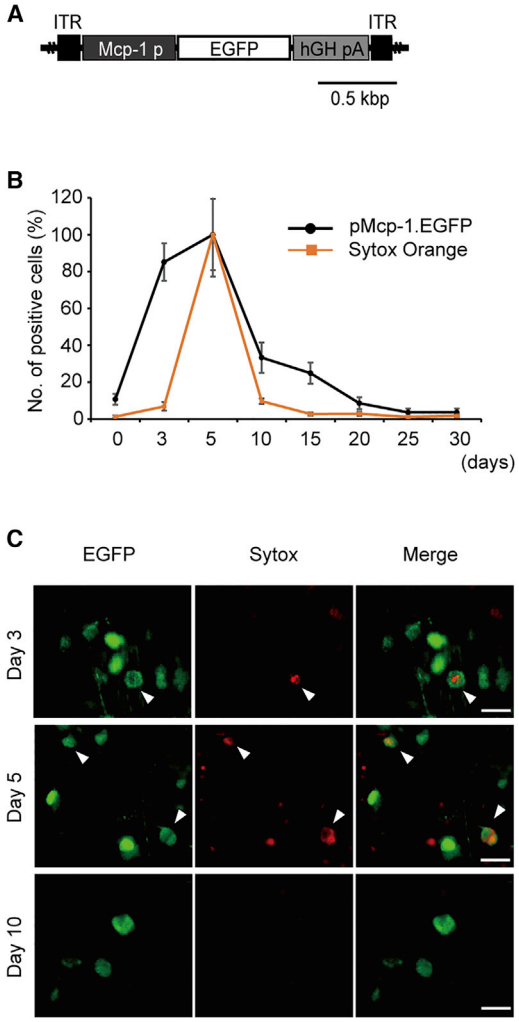

Figure 1. Temporal Profile of Mcp-1 Promoter Transcription Activity and RGC Death following Murine ONC

(A) Schematic representation of the AAV2/2 construct. The Mcp-1 promoter was designed to drive EGFP reporter gene expression (pMcp-1.EGFP). (B) Quantification of EGFP-positive cells and dying cells labeled with Sytox Orange each in a different group of mice (N = 8 for each group) before ONC and 5, 10, 15, and 20 days after injury. Images were obtained using in vivo confocal microscopy. The y axis indicates the number of Sytox-positive or EGFP-positive cells relative to that of the same mouse 5 days after ONC, presented in percentages. The x axis designates days after ONC. (C) Retinal flat mount prepared at 1, 5, and 10 days after ONC, showing colocalization of EGFP driven by the Mcp-1 promoter and Sytox Orange following ONC. Colocalization of Sytox Orange and EGFP is not seen at day 10. The arrowheads designate Sytox-positive cells in which Mcp-1 promoter is activated. Vector was injected at 2.0 μL (1.0×10^{12} gc/mL) per injection. ITR, inverted terminal repeat; hGHpA, human growth hormone polyadenylation signal. EGFP (green), Sytox Orange (red). Scale bar, 20 μm.

NRF2 to achieve spatially and temporally coordinated neuroprotection in a murine model of ONC to overcome the potential off-target toxicity of constitutive promoter-mediated gene therapy on healthy RGCs.

RESULTS

Upregulation of Mcp-1 Promoter Transcription Parallels RGC Death

We previously demonstrated that the Mcp-1 promoter is activated before detectable early apoptotic changes in a murine ONC model and that Mcp-1 promoter activation occurs mostly in RGCs.[15] However, whether Mcp-1 promoter activity increases and returns to baseline in parallel with RGC death is unknown. Following intravitreal injection of an EGFP-based reporter AAV2 driven by the Mcp-1 promoter (AAV2/2.pMcp-1.GFP) (Figure 1A), Sytox Orange, a fluorescent cell death marker amenable to in vivo real-time imaging, was used to assess the temporal profile of Mcp-1 promoter activation in relation to RGC death following ONC (Figure 1B). We found that upregulation of Mcp-1 promoter activity preceded RGC death triggered by injury, as previously reported,[15] and returned to baseline by 20 days after injury, in parallel with cessation of RGC death. Microscopic study revealed that some cells transcribing Mcp-1-EGFP also expressed Sytox Orange at 5 days after injury, consistent with the direct association of the Mcp-1-mediated stress response with RGC death (Figure 1C). In a similar experiment, colocalization of Sytox Orange and CMV promoter-driven EGFP was observed, indicating that CMV promoter is also used in injured cells (Figure S1).

Mcp-1 Promoter Driven Overexpression of BDNF or NRF2 Reduces RGC Death following Murine ONC

Next, we assessed the utility of the Mcp-1 promoter for effective gene therapy following murine ONC. Two AAV2 constructs were made carrying either human *BDNF* or *NRF2* driven by the Mcp-1 promoter (AAV2/2.pMcp-1.BDNF and AAV2/2.pMcp-1.NRF2) (Figure 2A). Both genes have been shown to prevent RGC death in retinal injury models using constitutive promoters.[18–20] Five days after ONC, expression levels of both Mcp-1 promoter-driven transgenes were elevated at the RNA level (Figure 2B) and the protein level (Figure 2C). Moreover, retinal cell death was reduced 46.2% by BDNF expression ($p = 0.0069$) and 62.1% by NRF2 overexpression ($p = 0.00037$) (Figure 2D). These findings were supported by expression analyses of constitutive RGC marker mRNAs (Brn3a, Brn3b, and Thy1), which showed higher levels in eyes treated with either construct compared to untreated control eyes. However, this effect was more consistent in mice treated with NRF2 compared to BDNF (Figure 2E). This may partially reflect the possible difference in the therapeutic effect size between the two vectors detected by in vivo cell death imaging (Figure 2D). Expression levels of all three markers were higher in eyes treated with AAV2/2.pMcp-1.NRF2, whereas only Brn3b expression was elevated following treatment with AAV2/2.pMcp-1.BDNF.

Early Stress-Responsive Mcp-1 Promoter-Driven and Constitutive CMV-Driven *NRF2* Overexpression Have Comparable Therapeutic Effects

Overexpression of the secreted protein BDNF by a subset of stressed RGCs could act on many surrounding RGCs. Alternatively, overexpression of NRF2, an intracellular transcription factor, would be

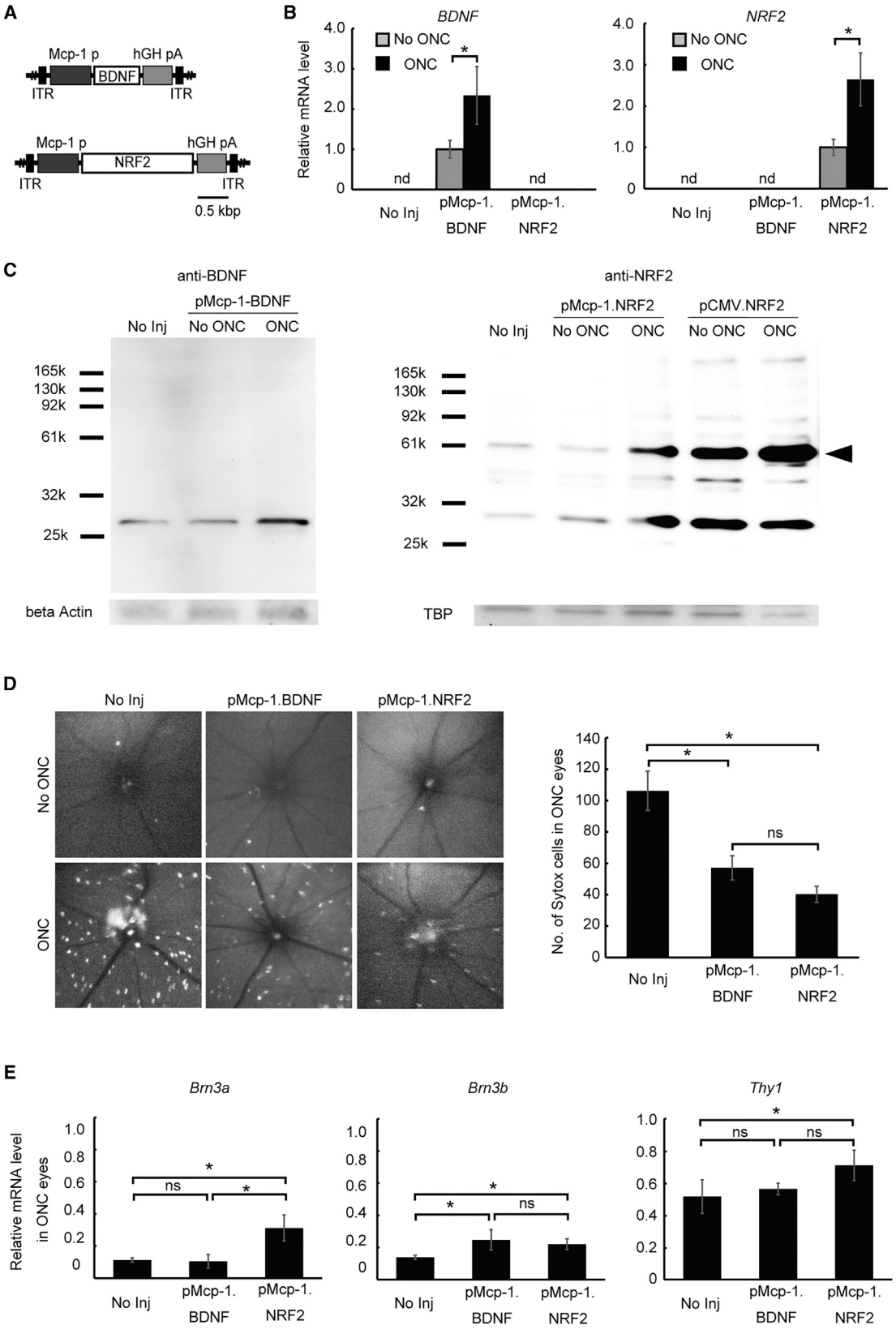

(legend on next page)

restricted to the subset of cells infected by the vector. Therefore, NRF2 was chosen as the therapeutic gene to explore the potential of temporally and spatially targeted gene therapy using the Mcp-1 promoter. To directly compare the therapeutic efficacy of a constitutive promoter (CMV) and the early stress-responsive Mcp-1 promoter, AAV vectors expressing NRF2 under the control of these promoters were generated (AAV2/2.pCMV.NRF2 and AAV2/2.pMcp-1.NRF2) (Figure 3A). Expression of *NRF2* confirmed by RT-PCR did not differ before and after ONC in the eyes treated with AAV2/2.pCMV.NRF2 (Figure 3B). This was different from the eyes treated with AAV2/2.pMcp-1.NRF2, which showed a 31.8-fold increase in *NRF2* expression following ONC (Figure 3B). The eyes treated with either of the two constructs showed lower numbers of dying RGCs after ONC injury than untreated contralateral control eyes as assessed by intravitreal Sytox Orange injection and imaging (Figure 3C). Furthermore, the therapeutic efficacies were similar for the two AAV2 vectors. However, expression levels of constitutive RGC markers were more consistently elevated by AAV2/2.pMcp-1.NRF2 (Figure 3D). To test the functional efficacy of these gene therapies, visual acuity and contrast sensitivity were measured after treatment. While we found no treatment effect on visual acuity using either vector 1 month post-ONC, both Mcp-1 and CMV promoter-driven NRF2 expression improved contrast sensitivity (52.2%, $p = 0.003$, and 66.7%, $p = 0.019$, respectively) with no difference in efficacy (percentage increase) between treatments (Figure 3E). The reason for the discrepancy between therapeutic effect on visual acuity and contrast sensitivity is unclear. However, the improvements in contrast sensitivity, but not in visual acuity, following treatment are not unprecedented.[21] It may reflect a modest therapeutic effect on the vision-guided behavior.

Constitutive Overexpression of NRF2 by the CMV Promoter Induces a Greater Stress Response in Healthy RGCs Than Overexpression by the Mcp-1 Promoter

We found that overexpression of NRF2 by the Mcp-1 promoter resulted in similar treatment efficacy to overexpression by CMV in a murine axonal injury model as assessed molecularly, histologically, and behaviorally. However, the Mcp-1 promoter is expected to be transcribed minimally in healthy cells, whereas the CMV promoter should be constitutively transcribed in both injured and healthy cells with no temporal and spatial specificity. This is of particular concern for clinical application, because indefinite overexpression of the target gene or genes in healthy cells will create a non-physiological intracellular environment that may lead to cell loss or disruption of function. Before testing this possibility, we first differentially measured the expression of endogenous *Nrf2* and exogenous *NRF2*. The endogenous *Nrf2* expression was not affected by the treatment of AAV2/2.pCMV.NRF2 or AAV2/2.pMcp-1.NRF2. However, we found a 44.4-fold increase in exogenous *NRF2* accompanied by a 5.3-fold increase in expression of *Ho-1*, a direct transcription target of NRF2, in the healthy eyes of wild-type mice treated with AAV2/2.pCMV.NRF2 compared to the healthy eyes treated with AAV2/2.pMcp-1.NRF2 (Figure 4A). Furthermore, expression levels of the endoplasmic reticulum stress marker *Aftf4* and the cell death pathway gene *p53* were elevated only in eyes treated with AAV2/2.pCMV.NRF2 compared to untreated eyes and eyes treated with AAV2/2.pMcp-1.NRF2 (Figure 4B). Meanwhile, expression of *Tgfb1* was elevated in the eyes treated with either vector. This result was confirmed by immunohistochemistry, which showed increased expression of Chop, indicating activation of endoplasmic reticulum stress, and p53, reflecting activation of a cell death pathway, in the ganglion cell layer (GCL) after treatment with AAV2/2.pCMV.NRF2 (Figure 4C). Similarly, expression levels of the stress markers *Hif1a* and *Nfkb1* were substantially upregulated by CMV promoter-driven NRF2 expression, not by Mcp-1 promoter-driven NRF2 expression, in healthy RGCs of untreated eyes.

Constitutive Expression of NRF2 by CMV Promoter Induces Stress Response that Could Be Diminished by Using MCP-1 Promoter

Next, we generated a bicistronic construct in which either the Mcp-1 promoter or the CMV promoter drives the simultaneous expression of NRF2 and EGFP to visually track NRF2 expression (AAV2/2.pMcp-1.NRF2-2A-EGFP and AAV2/2.pCMV.NRF2-2A-EGFP) over time in uninjured RGCs (Figure 5A). After injecting these constructs into the healthy eyes of wild-type mice, we monitored the number of transduced (EGFP emitting) cells periodically over the ensuing 8 months by in vivo ophthalmoscopy (Figures 5B and 5C). As expected, in the absence of axonal injury, the Mcp-1 promoter induced barely detectable EGFP expression, indicating low background promoter activity, while injection of the CMV promoter resulted in numerous EGFP-positive cells in uninjured eyes. Most importantly, the number of EGFP-positive cells gradually decreased over 1–8 months (~36.3% reduction; Cochran-Armitage trend test, $p = 0.025$) (Figures 5B and 5C). This was in contrast with the AAV2/2.CMV.EGFP-treated eyes, which showed no decline of EGFP-positive cells during the same period. The result indicates

Figure 2. Therapeutic Utilities of Mcp-1 Promoter-Driven BDNF and NRF2 Overexpression in Murine ONC

(A) Schematic representation of the AAV2/2 constructs. Construct carried BDNF (pMcp-1.BDNF) or NRF2 (pMcp-1.NRF2) as the therapeutic gene driven by the Mcp-1 promoter. (B) qRT-PCR analysis of therapeutic gene expression levels 5 days after injury. The graphs show relative mRNA expression levels in ONC eyes compared to non-treated contralateral eyes (N = 8 per group). (C) Typical western blots using antibodies against human BDNF (left) or NRF2 (right) 5 days after ONC. The 66 kDa band (arrowhead) represents uncleaved NRF2, while the lower band (30 kb) is its cleaved fragment. β-actin and TATA-box binding protein (TBP) were used as internal controls. (D) Representative in vivo confocal images of cell death visualized with Sytox Orange 5 days after ONC. The upper panels are images from control eyes, whereas the lower panels are images from the ONC eyes. Quantification of Sytox-positive RGCs from in vivo images (right; N = 10 per group). (E) qRT-PCR analysis of RGC marker genes. The graphs show levels of mRNA expression in ONC eyes. Values are expressed relative to the non-treated eye 7 days after ONC (N = 8 per group). Each vector was injected at 2.0 μL (1.0×10^{12} gc/mL) per injection for all experiments. Data represent means ± SEM, *$p < 0.05$. ITR, inverted terminal repeat; hGHpA, human growth hormone polyadenylation signal; No Inj, no injection; ND, non-detectable; NS, not significant.

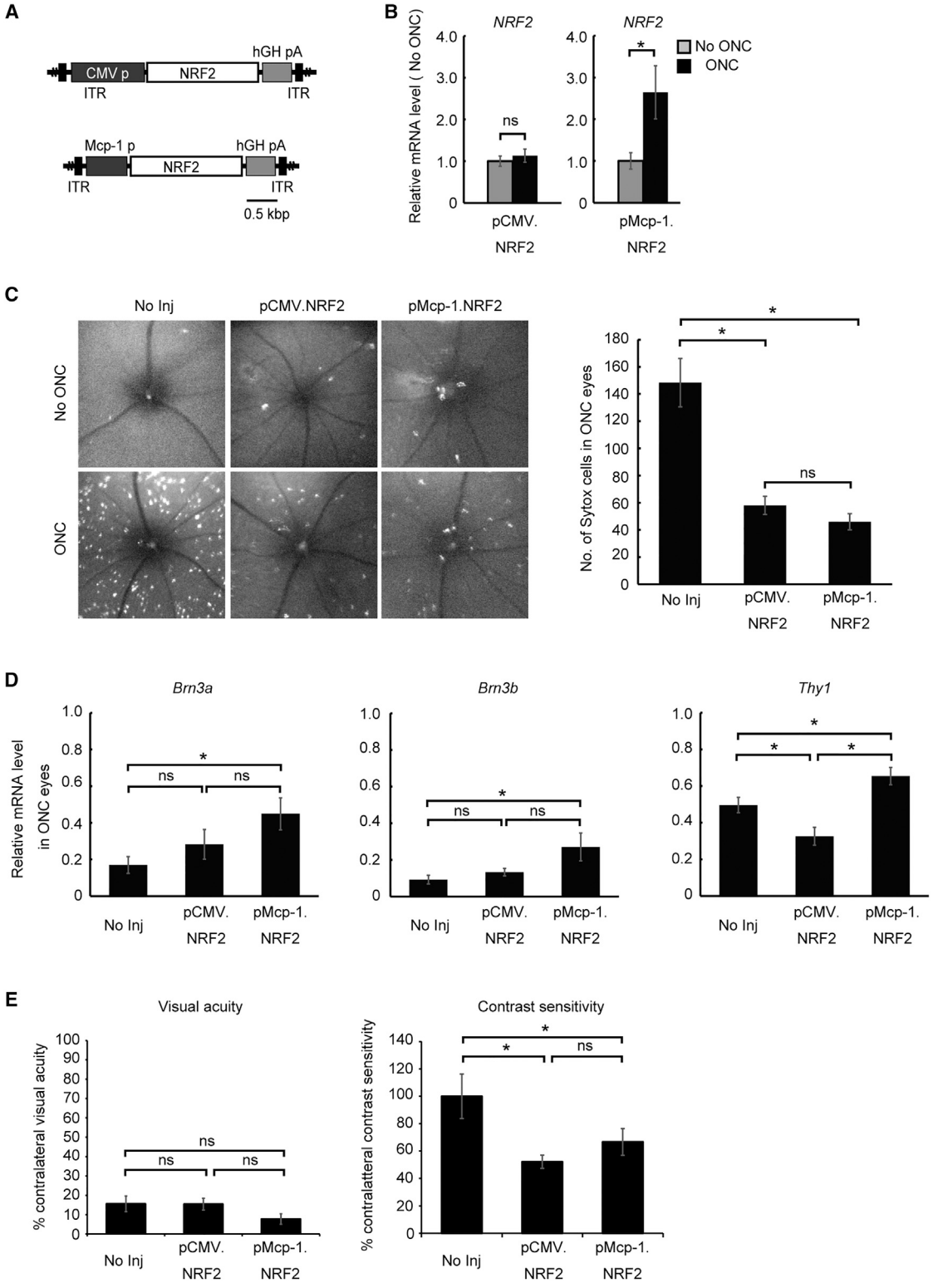

Figure 3. Comparison of Therapeutic Efficacy between CMV Promoter- and Mcp-1 Promoter-Driven NRF2 Expression in Murine ONC

(A) Schematic representation of the AAV2/2 constructs. Each construct carried NRF2 as the therapeutic gene driven by either the CMV promoter (pCMV.NRF2) or the Mcp-1 promoter (pMcp-1.NRF2). (B) qRT-PCR analysis of human NRF2 gene expression 5 days after injury. The graphs show mRNA expression levels in the ONC eyes relative to

(legend continued on next page)

that the NRF2 overexpression induces degeneration of RGCs. To distinguish these possibilities, we first compared the mRNA expression levels of RGC markers Brn3a, Brn3b, and Thy1 2 months after treating healthy wild-type mice with either AAV2/2.pMcp-1.NRF2 or AAV2/2.pCMV.NRF2 (Figure 5D). There was no difference in the expression levels of Brn3b and Thy1 between the two treatment groups (Figure 5E). However, the expression of Brn3a was reduced by 20.8% in eyes treated with the constitutive promoter (AAV2/2.pCMV.NRF2). We confirmed that this decrease was due to a specific reduction of BRN3A-positive RGCs through immunohistochemistry and comparative quantification of BRN3A-positive cells and DAPI-positive cells in retinal sections at 4 months (Figure 5F).

DISCUSSION

In this study, we found that AAV-mediated overexpression of the therapeutic transcription factor NRF2 driven by the early stress-responsive Mcp-1 promoter rescued RGCs in ONC model mice while minimizing undesired off-target effects on healthy RGCs associated with constitutive promoters. The use of a stress-responsive promoter provides a substantial advantage over a constitutive promoter for gene therapy of many chronic diseases in which damaged and healthy cells are intermixed within the same tissue. Therefore, Mcp-1 promoter-driven therapy may be effective for a variety of ocular and non-ocular conditions.

The finding that the rescue effect of AAV2/2.pMcp-1.NRF2 following ONC was more consistent compared to AAV2/2.pCMV.NRF2 was unexpected. Although the mechanism by which such a difference occurs is largely unknown, the negative off-target effects of AAV2/2.pCMV.NRF2 on RGCs, as shown in Figures 4 and 5, could have contributed the result. Likewise, the reason NRF2 overexpression is toxic to Brn3a-expressing cells, but not Brn3b-expressing cells, is not clear. Highly homologous POU-domain Brn3a and Brn3b transcription factors share identical transcriptional features. However, the functional roles of these transcription factors in RGCs differ, possibly because of the cell types in which the protein is expressed.[22] Expression of p53 known to strongly inhibit Brn3a-mediated expression of the Bcl-2 proto-oncogene that protects neuronal cells from programmed cell death[23] was elevated in the eyes overexpressing NRF2. This may have partly contributed to the death of Brn3a-positive RGCs.

Accumulating clinical evidence indicates that oxidative stress is a key pathogenic process in many chronic conditions affecting the retina, including age-related macular degeneration (AMD),[24,25] diabetic retinopathy,[25,26] retinitis pigmentosa,[27] and glaucoma,[3,28], which together account for most blindness cases in developed countries. These clinical findings are well supported by basic research on animal models of these conditions, which have provided evidence for the involvement of oxidative stress and the therapeutic potential of antioxidant therapy.[29] However, epidemiological studies have shown that simple oral intakes of antioxidative nutrients are not free of systemic side effects. For example, intake of vitamin E, an antioxidant, at a dose shown to be effective for preventing AMD has been linked to increased risk of prostate cancer.[30] Such evidence of deleterious non-target effects provides compelling rationale to restrict the therapeutic gene or agent to a defined tissue or cell subset. Gene therapy allowing local and long-term expression could be a particularly attractive approach for chronic intractable diseases. Others have demonstrated the therapeutic efficacy of AAV-mediated NRF2 delivery in murine models of retinitis pigmentosa and ONC.[18] Likewise, the concept of driving the antioxidative *Nrf2* gene by an early stress-inducible promoter should be effective for treating many ocular diseases other than glaucoma, because off-target expression of transgenes and associated long-term toxicity is a significant concern for most chronic ocular conditions. Mcp-1, a soluble chemokine that can be detected from patient ocular fluid samples, is a sensitive marker for the stress response of ocular cells in many chronic ocular conditions. Elevated protein expression levels, reflecting increased transcription of the Mcp-1 promoter, have been demonstrated in ocular fluid samples from patients with chronic blinding ocular diseases, including AMD,[31,32] diabetic retinopathy,[33] uveitis,[34] retinal detachment,[35–37] and retinitis pigmentosa.[38] Likewise, increased MCP-1 in the aqueous humor has been reported in glaucoma.[39,40] Although the cellular source of this increased MCP-1 remains undetermined, robust expression in multiple disorders suggests that the Mcp-1 promoter used in the current study could be broadly applicable for early stress-responsive gene therapy in many blinding diseases, including glaucoma.

The utility of inducible promoters, including drug-inducible promoters, is well recognized in the ocular field.[41–44] However, successful in vivo application of such promoters in animal models of ocular disease and neurodegeneration is rare. A successful in vivo application of a hypoxia-inducible promoter for treatment of ischemic retinopathy models has been reported.[45] Similarly, the utility has been reported in the murine middle cerebral artery occlusion model.[46] In that model, the hypoxia response element coupled to the *BDNF* gene delivered into the ipsilateral caudate-putamen reduced infarct volume.

In conclusion, Mcp-1 promoter-driven NRF2 overexpression only in stressed RGCs efficiently prevented degeneration following nerve crush injury while substantially reducing the off-target death of healthy neighboring RGCs. This approach is versatile and potentially

contralateral control (No ONC) eyes (N = 8 per group). (C) Representative images of cell death visualized by Sytox Orange 5 days after ONC using in vivo confocal microscopy (left panel). The upper panels are images from control eyes, and the lower panels are from ONC eyes. Quantification of Sytox-positive RGCs (right panel; N = 8 per group). (D) qRT-PCR analysis of RGC marker genes. The graphs show levels of mRNA expression in ONC eyes relative to contralateral eyes 7 days after ONC (N = 8 per group). (E) Measurement of visual acuity (left panel) and contrast sensitivity (right panel) 1 month after ONC (N = 6 per group). Each vector was injected at 2.0 μL (1.0×10^{12} gc/mL) per injection for all experiments. Data represent mean ± SEM, *$p < 0.05$. ITR, inverted terminal repeat; hGHpA, human growth hormone polyadenylation signal; No Inj, no injection; NS, not significant.

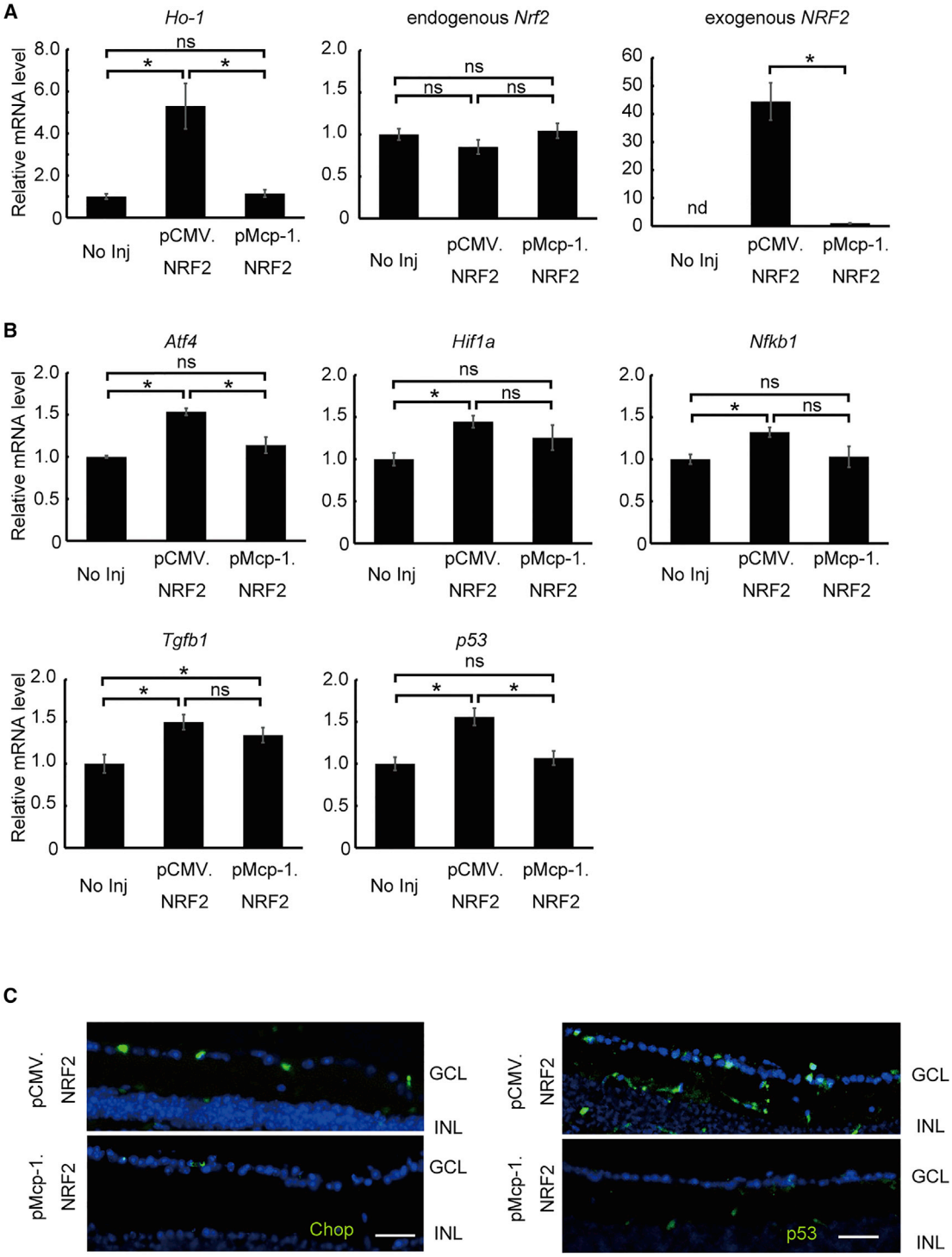

Figure 4. Off-Target Effects of NRF2 Expression Driven by the Mcp-1 Promoter versus CMV Promoter in Healthy RGCs of Wild-Type Mice

(A) qRT-PCR analysis of *Ho-1* gene expression in wild-type mice treated or untreated with a therapeutic vector (AAV2/2.pCMV.NRF2 or AAV2/2.pMcp-1.NRF2). *Ho-1* expression is regulated by NRF2 (N = 8 per group). (B) qRT-PCR analysis of RGC marker genes in wild-type mice treated or untreated with therapeutic vector. The graphs show levels of mRNA expression in the retina 2 months after AAV injection relative to the contralateral untreated eyes (N = 8 per group). (C) Representative images of retinal section immunoreactivity for Chop (left) and p53 (right) 2 months after AAV injection. Each vector was injected at 2.0 μL (1.0×10^{12} gc/mL) per injection for all experiments. All data represent means ± SEM, *$p < 0.05$. GCL, ganglion cell layer; INL, inner nuclear layer; No Inj, no injection; NS, not significant. Scale bar, 50 μm.

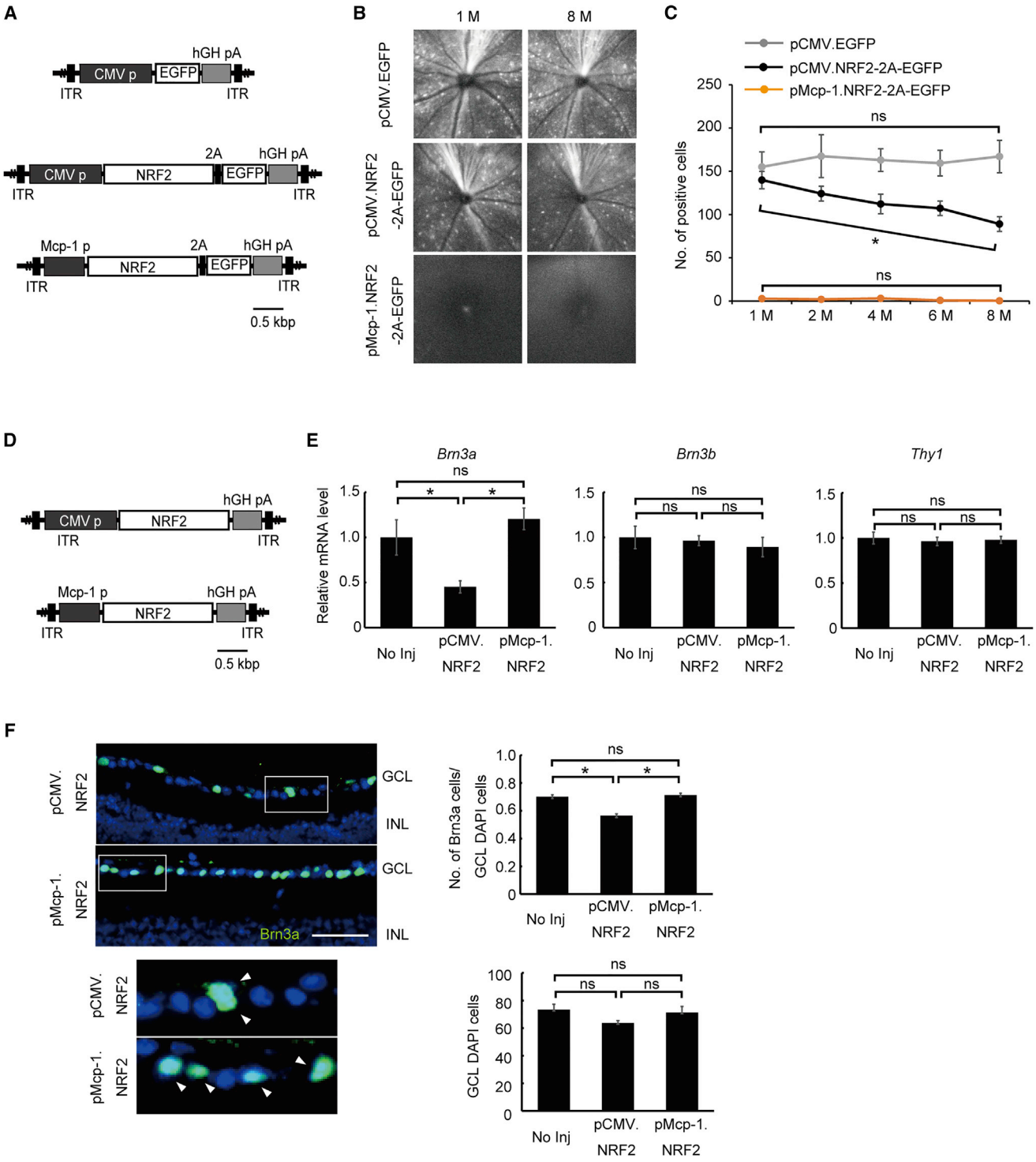

Figure 5. Comparative Evaluation of Toxicity from NRF2 Expression Driven by the CMV or Mcp-1 Promoter in Healthy RGCs in Wild-Type Mice

(A) Schematic representation of the AAV2/2 vectors used in (B) and (C). Bicistronic constructs were composed of the Mcp-1 promoter (pMcp-1.NRF2-2A-EGFP) or CMV promoter (pCMV.NRF2-2A-EGFP) driving NRF2 connected to EGFP via the self-cleaving peptide (2A). (B) Representative in vivo images of NRF2-expressing EGFP-positive cells (RGCs) in wild-type mice 1, 4, and 8 months after AAV injection obtained using confocal microscopy. (C) Quantification of NRF2-expressing EGFP-positive RGCs from in vivo images (N = 5 each). (D) Schematic representation of the AAV2/2 constructs used in (E) and (F). Each construct carried NRF2 as the therapeutic gene driven by either

(legend continued on next page)

could be applied to many other conditions in which oxidative stress plays a central pathogenic role.

MATERIALS AND METHODS

Animals

This study used adult (6- to 32-week-old) male C57BL/6J mice (Japan SLC). The animals were housed in a 14 hr light and 10 hr dark cycle with free access to food and water. Surgical procedures were performed under deep anesthesia induced by intraperitoneal administration of a mixture of ketamine (37.5 mg/kg) and medetomidine (0.625 mg/kg). The medetomidine effect was reversed by intraperitoneal injection of 1 atipamezole (.25 mg/kg). All mice were handled and maintained in accordance with the Association for Research in Vision and Ophthalmology (ARVO) guidelines for the Use of Animals in Ophthalmic and Vision Research and intramural guidelines for the care and use of animals. All experimental procedures were conducted after approval by the ethics committee for animal experiments at the Tohoku University Graduate School of Medicine. Mice were masked before any quantification to limit subjective bias. Animals were randomly assigned to AAV-treatment or no-treatment groups from a given litter of mice. The contralateral eye served as internal control to which no treatment was indicated partly, because there were no differences in RT-PCR of RGC marker expression between the eyes with no treatment and those treated with AAV2/2.pCMV.EGFP following ONC (Figure S2). The estimate of sample size was calculated with an animal experimentation sample size calculator (http://www.lasec.cuhk.edu.hk/sample-size-calculation.html).

Axonal Injury

ONC to induce axonal injury in RGCs was performed as described previously.[47] In brief, the optic nerve was exposed while avoiding the blood vessel and was crushed approximately 2 mm posterior to the eyeball with forceps for 5 s. Several minutes after ONC, normal retinal circulation was confirmed through direct observation of the fundus. Antibiotic ointment was then applied to the treated eye.

AAV Construction

To construct pMcp-1.BDNF and pMcp-1.NRF2 vectors, a fragment of the murine Mcp-1 promoter (560 bp immediately upstream of the initiation codon ATG; accession number U12470) and BDNF cDNA (KIBB9810; Promega) or NRF2 cDNA (KIBB7828; Promega) were inserted into a pAAV-MCS Promoterless Expression Vector (Cell Biolabs). To construct pMcp-1.NRF2-2A-EGFP, the same fragment of the Mcp-1 promoter, NRF2 cDNA, linker peptide 2A cDNA, and *EGFP* cDNA (Clontech) were inserted into the pAAV-MCS Promoterless Expression Vector using the Gibson assembly system (New England Biolabs). To construct pCMVNRF2-2A-EGFP, *Nrf2* cDNA, 2A peptide, and *egfp* cDNA (Clontech) were inserted into a pAAV-CMVp-MCS Expression Vector (Cell Biolabs) using the Gibson assembly system (New England Biolabs). For pAAV.CMV.EGFP using pAAV-GFP vector (Cell Biolabs), viral vectors AAV2/2 were generated and purified following a method described previously.[48] Each vector (1.0×10^{12} genome copy [gc]/mL) was injected at 2.0 μL per injection into the vitreous of an anaesthetized mouse. The dose was the same in all experiments involving intravitreal injection of AAV in this study.

In Vivo Cellular Imaging

Cell death labeling was performed using Sytox Orange (Life Technologies) as described previously.[49] Sytox Orange (2.5 nM) was injected intravitreally at 1.0 μL/injection. Images were acquired using confocal ophthalmoscopy (Nidek F10; Nidek) 10 min post-injection as described previously.[15] Briefly, mice were anaesthetized and pupils were dilated with 2.5% phenylephrine and 1.0% tropicamide. Blue laser light (488 nm) was used for EGFP excitation, and a band path filter set to 510–550 nm was used to capture emission. Green laser light (532 nm) was used for excitation, and a barrier filter set at a cut-off of 555 nm was used to capture Sytox Orange emission. Clear distinction between signals from Sytox Orange and EGFP was not possible. The focus was adjusted at the RGC layer in the posterior pole immediately posterior to the retinal surface. Six raw images were averaged to obtain an image of the posterior pole, with the optic nerve head aligned in the center for analysis. The number of fluorescent cells was quantified from a single image at a given time point per mouse by an observer blinded to treatment history.

qRT-PCR

Total RNA was extracted from the retina using the miRNeasy Plus Mini Kit (QIAGEN) according to the manufacturer's instructions. One microgram of total RNA was reverse transcribed in a 10 μL reaction mixture using SuperScript III (Thermo Fisher Scientific), and qRT-PCR was performed (7500 Fast Real-Time PCR System; Thermo Fisher Scientific). The 20 μL qRT-PCR mixture contained 1.0 μL of cDNA, 1.0 μL of TaqMan probe (Thermo Fisher Scientific), and 1× TaqMan Fast Universal PCR Master mix (Thermo Fisher Scientific). PCR was performed in 96-well plates using an initial denaturation step of 95°C for 20 s, followed by 40 cycles of 95°C for 3 s and 60°C for 20 s. For relative comparison of gene expression, we analyzed qRT-PCR data using the comparative Ct method (2-ΔΔCT) normalized to *Gapdh* as the endogenous control. The following TaqMan probes were used: *Atf4* (Mm00515324; Thermo Fisher Scientific), *BDNF* (Hs02718934; Thermo Fisher Scientific), *Ho-1* (Mm00516005; Thermo Fisher Scientific), *Nfkb1* (Mm00476379; Thermo Fisher Scientific), *NRF2* (Hs00975961;

the CMV promoter (pCMV.NRF2) or the Mcp-1 promoter (pMcp-1.NRF2). (E) qRT-PCR analysis of RGC marker genes in wild-type mice treated or untreated with a therapeutic vector. The graphs show mRNA expression levels in the retina 2 months after AAV injection relative to the contralateral untreated eyes (N = 8 each). (F) Immunohistochemical analysis of retinal sections stained with anti-Brn3a antibodies (green) 4 months after AAV injection (left), with highly magnified images shown in insets. Graphs show quantification of Brn3a-positive cells per DAPI-positive cells (center; N = 6 each) and DAPI-positive cells (right; N = 6 each) in the GCL from images. Each vector was injected at 2.0 μL (1.0×10^{12} gc/mL) per injection for all experiments. All data represent means ± SEM. *$p < 0.05$ with Cochran-Armitage test for trend. GCL, ganglion cell layer; INL, inner nuclear layer; 2A, self-cleaving peptide; ITR, inverted terminal repeat; hGHpA, human growth hormone polyadenylation signal. Scale bar, 50 μm.

Thermo Fisher Scientific), *Gapdh* (Mm99999915; Thermo Fisher Scientific), *Brn3a* (Mm02343791; Thermo Fisher Scientific), *Brn3b* (Mm00454754; Thermo Fisher Scientific), *Thy1* (Mm00493681; Thermo Fisher Scientific), *Tgfb1* (Mm00441729; Thermo Fisher Scientific), and *p53* (Mm01731290; Thermo Fisher Scientific).

Western Blot

Isolated mouse retina was lysed in a radioimmunoprecipitation (RIPA) buffer supplemented with a protease inhibitor (Roche) by two 30 s sonications on ice. Nuclear proteins were isolated using a Nuclear Extraction Kit (Abcam) according to the manufacturer's instructions. Total protein concentration was measured with the Pierce bicinchoninic acid (BCA) protein assay kit (Thermo Fisher Scientific). Mouse retinal proteins (15 μg each) were separated by SDS-PAGE on 4%–15% gradient gels (Bio-Rad) and transferred to polyvinylidene fluoride (PVDF) membranes (Millipore). The membranes were blocked in 5% milk/phosphate buffered saline with tween 20 (PBS-T) for 1 hr and then incubated with antibodies against BDNF (AB1513, 1/1,000; Millipore), NRF2 (sc-13032, 1/1,000; Santa Cruz Biotechnology), β-actin (F5316, 1/2,000; Sigma-Aldrich), and TBP (#8515, 1/1,000; Cell Signaling Technology) for 1 hr. Immunolabeled membranes were washed three times with PBS-T for 10 min each, incubated with horseradish peroxidase (HRP)-conjugated anti-rabbit immunoglobulin G (IgG) antibodies (A0545, 1/2,000; Sigma-Aldrich) for 1 hr, and then washed four times for 5 min each with PBS-T. The immunogenic reaction was detected by ECL Prime (GE Healthcare).

Immunohistochemistry

Eyes were fixed in 4% paraformaldehyde, embedded in optical coherence tomography (OCT) compound (Sakura Finetek), and sectioned using a cryostat (CM3050; Leica Microsystems). The section was blocked with 5% donkey serum for 30 min, incubated with goat anti-Brn3a antibody (sc-31984, 1:100; Santa Cruz Biotechnology), mouse anti-chop antibody (#2895, 1:500; Cell Signaling Technology), or rabbit anti-p53 antibody (sc-6243, 1:100; Santa Cruz Biotechnology) for 1 hr and then stained with an appropriate secondary antibody (anti-goat Alexa Fluor 488, anti-rabbit Alexa Fluor 488, or anti-mouse Alexa Fluor 488; Thermo Fisher Scientific) and DAPI (Vector Labs) for an additional 45 min. For primary antibodies raised in mice, frozen sections were treated in using the Mouse on Mouse Immunodetection kit (BMK-2202, Vector Labs) according to the manufacturer's instructions. Cells in the GCL were counted in a 1 mm^2 area on each side of the optic nerve under a 20× objective in five 60-μm-spaced sections from each retina.

Optomotry

Visual acuities and contrast sensitivity were measured by observing the optokinetic responses of mice to rotating sinusoidal gratings (OptoMotry, Cerebral Mechanics)[50] as described previously.[48] The protocol yields independent measures of right and left eye acuity based on unequal sensitivities to pattern rotation direction, as the motion in the temporal-to-nasal direction dominates the tracking response.[48] Mice were housed under standard lighting conditions for at least 6 hr before they were placed in the recording chamber. Visual acuity and contrast sensitivity reported for each eye are the averages of four trials conducted on separate days.

Statistical Analysis

Differences between two groups were assessed using unpaired Student's t test. A p value of <0.05 was inferred as significant. The Cochran-Armitage test ($p < 0.05$) was applied to assess increasing or decreasing trends in the number of EGFP-positive cells during the 8 months after treatment (Figure 5C) using R (http://www.R-project.org). Normal distribution was assessed by Kolmogorov-Smirnov test using R. All values are expressed as mean ± SEM.

SUPPLEMENTAL INFORMATION

Supplemental Information includes two figures and can be found with this article online at http://dx.doi.org/10.1016/j.omtm.2017.04.003.

AUTHOR CONTRIBUTIONS

K.F. and K.M.N. wrote the manuscript. K.F. performed most of the experiments. Y.S. and T.N. helped with the animal experiments. K.F., K.M.N., and T.N. obtained the funding.

CONFLICTS OF INTEREST

The authors have no conflict of interest.

ACKNOWLEDGMENTS

This work was supported in part by JSPS KAKENHI Grants-in-Aid for Scientific Research C (16K11315 to K.M.N.) and for Young Scientists B (16K20301 to K.F.), the 2016 Charitable Trust Fund for Ophthalmic Research in Commemoration of Santen Pharmaceutical's Founder (to K.M.N.), the Japan National Society for the Prevention of Blindness (to K.M.N.), and the Fund by Senju Pharma Co. (to K.M.N. and T.N.). We used Enago Co. Ltd. (http://www.enago.jp/) for English editing and proofreading service.

REFERENCES

1. Quigley, H.A., Addicks, E.M., and Green, W.R. (1982). Optic nerve damage in human glaucoma. III. Quantitative correlation of nerve fiber loss and visual field defect in glaucoma, ischemic neuropathy, papilledema, and toxic neuropathy. Arch. Ophthalmol. *100*, 135–146.

2. Izzotti, A., Saccà, S.C., Cartiglia, C., and De Flora, S. (2003). Oxidative deoxyribonucleic acid damage in the eyes of glaucoma patients. Am. J. Med. *114*, 638–646.

3. Ferreira, S.M., Lerner, S.F., Brunzini, R., Evelson, P.A., and Llesuy, S.F. (2004). Oxidative stress markers in aqueous humor of glaucoma patients. Am. J. Ophthalmol. *137*, 62–69.

4. Chang, D., Sha, Q., Zhang, X., Liu, P., Rong, S., Han, T., Liu, P., and Pan, H. (2011). The evaluation of the oxidative stress parameters in patients with primary angle-closure glaucoma. PLoS ONE *6*, e27218.

5. Himori, N., Kunikata, H., Shiga, Y., Omodaka, K., Maruyama, K., Takahashi, H., and Nakazawa, T. (2016). The association between systemic oxidative stress and ocular blood flow in patients with normal-tension glaucoma. Graefes Arch. Clin. Exp. Ophthalmol. *254*, 333–341.

6. Moreno, M.C., Campanelli, J., Sande, P., Sánez, D.A., Keller Sarmiento, M.I., and Rosenstein, R.E. (2004). Retinal oxidative stress induced by high intraocular pressure. Free Radic. Biol. Med. *37*, 803–812.

7. Tezel, G., Yang, X., and Cai, J. (2005). Proteomic identification of oxidatively modified retinal proteins in a chronic pressure-induced rat model of glaucoma. Invest. Ophthalmol. Vis. Sci. *46*, 3177–3187.
8. Levkovitch-Verbin, H., Harris-Cerruti, C., Groner, Y., Wheeler, L.A., Schwartz, M., and Yoles, E. (2000). RGC death in mice after optic nerve crush injury: oxidative stress and neuroprotection. Invest. Ophthalmol. Vis. Sci. *41*, 4169–4174.
9. Himori, N., Yamamoto, K., Maruyama, K., Ryu, M., Taguchi, K., Yamamoto, M., and Nakazawa, T. (2013). Critical role of Nrf2 in oxidative stress-induced retinal ganglion cell death. J. Neurochem. *127*, 669–680.
10. Hauswirth, W.W., Aleman, T.S., Kaushal, S., Cideciyan, A.V., Schwartz, S.B., Wang, L., Conlon, T.J., Boye, S.L., Flotte, T.R., Byrne, B.J., and Jacobson, S.G. (2008). Treatment of Leber congenital amaurosis due to RPE65 mutations by ocular subretinal injection of adeno-associated virus gene vector: short-term results of a phase I trial. Hum. Gene Ther. *19*, 979–990.
11. Bainbridge, J.W., Smith, A.J., Barker, S.S., Robbie, S., Henderson, R., Balaggan, K., Viswanathan, A., Holder, G.E., Stockman, A., Tyler, N., et al. (2008). Effect of gene therapy on visual function in Leber's congenital amaurosis. N. Engl. J. Med. *358*, 2231–2239.
12. Maguire, A.M., Simonelli, F., Pierce, E.A., Pugh, E.N., Jr., Mingozzi, F., Bennicelli, J., Banfi, S., Marshall, K.A., Testa, F., Surace, E.M., et al. (2008). Safety and efficacy of gene transfer for Leber's congenital amaurosis. N. Engl. J. Med. *358*, 2240–2248.
13. MacLaren, R.E., Groppe, M., Barnard, A.R., Cottriall, C.L., Tolmachova, T., Seymour, L., Clark, K.R., During, M.J., Cremers, F.P., Black, G.C., et al. (2014). Retinal gene therapy in patients with choroideremia: initial findings from a phase 1/2 clinical trial. Lancet *383*, 1129–1137.
14. Rakoczy, E.P., Lai, C.M., Magno, A.L., Wikstrom, M.E., French, M.A., Pierce, C.M., Schwartz, S.D., Blumenkranz, M.S., Chalberg, T.W., Degli-Esposti, M.A., and Constable, I.J. (2015). Gene therapy with recombinant adeno-associated vectors for neovascular age-related macular degeneration: 1 year follow-up of a phase 1 randomised clinical trial. Lancet *386*, 2395–2403.
15. Fujita, K., Nishiguchi, K.M., Yokoyama, Y., Tomiyama, Y., Tsuda, S., Yasuda, M., Maekawa, S., and Nakazawa, T. (2015). In vivo cellular imaging of various stress/response pathways using AAV following axonal injury in mice. Sci. Rep. *5*, 18141.
16. Toney, L.M., Cattoretti, G., Graf, J.A., Merghoub, T., Pandolfi, P.P., Dalla-Favera, R., Ye, B.H., and Dent, A.L. (2000). BCL-6 regulates chemokine gene transcription in macrophages. Nat. Immunol. *1*, 214–220.
17. Itoh, K., Chiba, T., Takahashi, S., Ishii, T., Igarashi, K., Katoh, Y., Oyake, T., Hayashi, N., Satoh, K., Hatayama, I., et al. (1997). An Nrf2/small Maf heterodimer mediates the induction of phase II detoxifying enzyme genes through antioxidant response elements. Biochem. Biophys. Res. Commun. *236*, 313–322.
18. Xiong, W., MacColl Garfinkel, A.E., Li, Y., Benowitz, L.I., and Cepko, C.L. (2015). NRF2 promotes neuronal survival in neurodegeneration and acute nerve damage. J. Clin. Invest. *125*, 1433–1445.
19. Di Polo, A., Aigner, L.J., Dunn, R.J., Bray, G.M., and Aguayo, A.J. (1998). Prolonged delivery of brain-derived neurotrophic factor by adenovirus-infected Müller cells temporarily rescues injured retinal ganglion cells. Proc. Natl. Acad. Sci. USA *95*, 3978–3983.
20. Leaver, S.G., Cui, Q., Plant, G.W., Arulpragasam, A., Hisheh, S., Verhaagen, J., and Harvey, A.R. (2006). AAV-mediated expression of CNTF promotes long-term survival and regeneration of adult rat retinal ganglion cells. Gene Ther. *13*, 1328–1341.
21. Woo, G.C., and Dalziel, C.C. (1981). A pilot study of contrast sensitivity assessment of the CAM treatment of amblyopia. Acta Ophthalmol. (Copenh.) *59*, 35–37.
22. Badea, T.C., Cahill, H., Ecker, J., Hattar, S., and Nathans, J. (2009). Distinct roles of transcription factors brn3a and brn3b in controlling the development, morphology, and function of retinal ganglion cells. Neuron *61*, 852–864.
23. Budhram-Mahadeo, V., Morris, P.J., Smith, M.D., Midgley, C.A., Boxer, L.M., and Latchman, D.S. (1999). p53 suppresses the activation of the Bcl-2 promoter by the Brn-3a POU family transcription factor. J. Biol. Chem. *274*, 15237–15244.
24. Eye Disease Case-Control Study Group (1993). Antioxidant status and neovascular age-related macular degeneration. Arch. Ophthalmol. *111*, 104–109.
25. Samiec, P.S., Drews-Botsch, C., Flagg, E.W., Kurtz, J.C., Sternberg, P., Jr., Reed, R.L., and Jones, D.P. (1998). Glutathione in human plasma: decline in association with aging, age-related macular degeneration, and diabetes. Free Radic. Biol. Med. *24*, 699–704.
26. Hartnett, M.E., Stratton, R.D., Browne, R.W., Rosner, B.A., Lanham, R.J., and Armstrong, D. (2000). Serum markers of oxidative stress and severity of diabetic retinopathy. Diabetes Care *23*, 234–240.
27. Martínez-Fernández de la Cámara, C., Salom, D., Sequedo, M.D., Hervás, D., Marín-Lambíes, C., Aller, E., Jaijo, T., Díaz-Llopis, M., Millán, J.M., and Rodrigo, R. (2013). Altered antioxidant-oxidant status in the aqueous humor and peripheral blood of patients with retinitis pigmentosa. PLoS ONE *8*, e74223.
28. Saccà, S.C., Pascotto, A., Camicione, P., Capris, P., and Izzotti, A. (2005). Oxidative DNA damage in the human trabecular meshwork: clinical correlation in patients with primary open-angle glaucoma. Arch. Ophthalmol. *123*, 458–463.
29. Rhone, M., and Basu, A. (2008). Phytochemicals and age-related eye diseases. Nutr. Rev. *66*, 465–472.
30. Klein, E.A., Thompson, I.M., Jr., Tangen, C.M., Crowley, J.J., Lucia, M.S., Goodman, P.J., Minasian, L.M., Ford, L.G., Parnes, H.L., Gaziano, J.M., et al. (2011). Vitamin E and the risk of prostate cancer: the Selenium and Vitamin E Cancer Prevention Trial (SELECT). JAMA *306*, 1549–1556.
31. Jonas, J.B., Tao, Y., Neumaier, M., and Findeisen, P. (2010). Monocyte chemoattractant protein 1, intercellular adhesion molecule 1, and vascular cell adhesion molecule 1 in exudative age-related macular degeneration. Arch. Ophthalmol. *128*, 1281–1286.
32. Jonas, J.B., Tao, Y., Neumaier, M., and Findeisen, P. (2012). Cytokine concentration in aqueous humour of eyes with exudative age-related macular degeneration. Acta Ophthalmol. *90*, e381–e388.
33. Elner, S.G., Elner, V.M., Jaffe, G.J., Stuart, A., Kunkel, S.L., and Strieter, R.M. (1995). Cytokines in proliferative diabetic retinopathy and proliferative vitreoretinopathy. Curr. Eye Res. *14*, 1045–1053.
34. Verma, M.J., Lloyd, A., Rager, H., Strieter, R., Kunkel, S., Taub, D., and Wakefield, D. (1997). Chemokines in acute anterior uveitis. Curr. Eye Res. *16*, 1202–1208.
35. Abu el-Asrar, A.M., Van Damme, J., Put, W., Veckeneer, M., Dralands, L., Billiau, A., and Missotten, L. (1997). Monocyte chemotactic protein-1 in proliferative vitreoretinal disorders. Am. J. Ophthalmol. *123*, 599–606.
36. Nakazawa, T., Hisatomi, T., Nakazawa, C., Noda, K., Maruyama, K., She, H., Matsubara, A., Miyahara, S., Nakao, S., Yin, Y., et al. (2007). Monocyte chemoattractant protein 1 mediates retinal detachment-induced photoreceptor apoptosis. Proc. Natl. Acad. Sci. USA *104*, 2425–2430.
37. Kunikata, H., Yasuda, M., Aizawa, N., Tanaka, Y., Abe, T., and Nakazawa, T. (2013). Intraocular concentrations of cytokines and chemokines in rhegmatogenous retinal detachment and the effect of intravitreal triamcinolone acetonide. Am. J. Ophthalmol. *155*, 1028–1037.e1.
38. Yoshida, N., Ikeda, Y., Notomi, S., Ishikawa, K., Murakami, Y., Hisatomi, T., Enaida, H., and Ishibashi, T. (2013). Clinical evidence of sustained chronic inflammatory reaction in retinitis pigmentosa. Ophthalmology *120*, 100–105.
39. Freedman, J., and Iserovich, P. (2013). Pro-inflammatory cytokines in glaucomatous aqueous and encysted Molteno implant blebs and their relationship to pressure. Invest. Ophthalmol. Vis. Sci. *54*, 4851–4855.
40. Inoue, T., Kawaji, T., Inatani, M., Kameda, T., Yoshimura, N., and Tanihara, H. (2012). Simultaneous increases in multiple proinflammatory cytokines in the aqueous humor in pseudophakic glaucomatous eyes. J. Cataract Refract. Surg. *38*, 1389–1397.
41. McGee Sanftner, L.H., Rendahl, K.G., Quiroz, D., Coyne, M., Ladner, M., Manning, W.C., and Flannery, J.G. (2001). Recombinant AAV-mediated delivery of a tet-inducible reporter gene to the rat retina. Mol. Ther. *3*, 688–696.
42. Lebherz, C., Auricchio, A., Maguire, A.M., Rivera, V.M., Tang, W., Grant, R.L., Clackson, T., Bennett, J., and Wilson, J.M. (2005). Long-term inducible gene expression in the eye via adeno-associated virus gene transfer in nonhuman primates. Hum. Gene Ther. *16*, 178–186.
43. Stieger, K., Le Meur, G., Lasne, F., Weber, M., Deschamps, J.Y., Nivard, D., Mendes-Madeira, A., Provost, N., Martin, L., Moullier, P., and Rolling, F. (2006). Long-term doxycycline-regulated transgene expression in the retina of nonhuman primates following subretinal injection of recombinant AAV vectors. Mol. Ther. *13*, 967–975.

44. Sochor, M.A., Vasireddy, V., Drivas, T.G., Wojno, A., Doung, T., Shpylchak, I., Bennicelli, J., Chung, D., Bennett, J., and Lewis, M. (2015). An autogenously regulated expression system for gene therapeutic ocular applications. Sci. Rep. *5*, 17105.

45. Biswal, M.R., Prentice, H.M., Dorey, C.K., and Blanks, J.C. (2014). A hypoxia-responsive glial cell-specific gene therapy vector for targeting retinal neovascularization. Invest. Ophthalmol. Vis. Sci. *55*, 8044–8053.

46. Shi, Q., Zhang, P., Zhang, J., Chen, X., Lu, H., Tian, Y., Parker, T.L., and Liu, Y. (2009). Adenovirus-mediated brain-derived neurotrophic factor expression regulated by hypoxia response element protects brain from injury of transient middle cerebral artery occlusion in mice. Neurosci. Lett. *465*, 220–225.

47. Ryu, M., Yasuda, M., Shi, D., Shanab, A.Y., Watanabe, R., Himori, N., Omodaka, K., Yokoyama, Y., Takano, J., Saido, T., and Nakazawa, T. (2012). Critical role of calpain in axonal damage-induced retinal ganglion cell death. J. Neurosci. Res. *90*, 802–815.

48. Nishiguchi, K.M., Carvalho, L.S., Rizzi, M., Powell, K., Holthaus, S.M., Azam, S.A., Duran, Y., Ribeiro, J., Luhmann, U.F., Bainbridge, J.W., et al. (2015). Gene therapy restores vision in rd1 mice after removal of a confounding mutation in Gpr179. Nat. Commun. *6*, 6006.

49. Tsuda, S., Tanaka, Y., Kunikata, H., Yokoyama, Y., Yasuda, M., Ito, A., and Nakazawa, T. (2016). Real-time imaging of RGC death with a cell-impermeable nucleic acid dyeing compound after optic nerve crush in a murine model. Exp. Eye Res. *146*, 179–188.

50. Prusky, G.T., Alam, N.M., Beekman, S., and Douglas, R.M. (2004). Rapid quantification of adult and developing mouse spatial vision using a virtual optomotor system. Invest. Ophthalmol. Vis. Sci. *45*, 4611–4616.